

1 **Title:** An Autonomous Flow Through Salinity and Temperature Perturbation Mesocosm System  
2 for Multi-stressor Experiments

3  
4 **Author list:** Cale A. Miller<sup>1,2\*</sup>, Pierre Urrutti<sup>1</sup>, Jean-Pierre Gattuso<sup>1,3</sup>, Steeve Comeau<sup>1</sup>, Anaïs  
5 Lebrun<sup>1</sup>, Samir Alliouane<sup>1</sup>, Robert W. Schlegel<sup>1</sup>, and Frédéric Gazeau<sup>1</sup>

6  
7 <sup>1</sup>Sorbonne Université, CNRS, Laboratoire d'Océanographie de Villefranche, 181 chemin du  
8 Lazaret, F-06230 Villefranche-sur-Mer, France

9  
10 <sup>2</sup>Present address: Department of Earth Sciences, Geosciences, Utrecht University, Utrecht, The  
11 Netherlands

12  
13 <sup>3</sup>Institute for Sustainable Development and International Relations, Sciences Po, 27 rue Saint  
14 Guillaume, F-75007 Paris, France

15  
16  
17 *\*Correspondence to:* Cale A. Miller (e-mail: [c.a.miller@uu.nl](mailto:c.a.miller@uu.nl))  
18  
19  
20  
21  
22  
23  
24  
25  
26  
27  
28  
29  
30  
31  
32  
33

34 **Abstract**

35 The rapid environmental changes in aquatic systems as a result of anthropogenic forcings are  
36 creating a multitude of challenging conditions for organisms and communities. The need to  
37 better understand the interaction of environmental stressors now, and in the future, is  
38 fundamental to determining the response of ecosystems to these perturbations. This work  
39 describes an automated *ex-situ* mesocosm perturbation system that can manipulate several  
40 variables of aquatic media in a controlled setting. This perturbation system was deployed in  
41 Kongsfjorden (Svalbard) where ambient water from the fjord was heated and mixed with  
42 freshwater in a multifactorial design to investigate the response of mixed kelp communities in  
43 mesocosms to projected future Arctic conditions. The system employed an automated dynamic  
44 offset scenario where a nominal temperature increase was programmed as a set value above real-  
45 time ambient conditions in order to simulate future warming. A freshening component was  
46 applied in a similar manner where a decrease in salinity was coupled to track the temperature  
47 offset based on a temperature-salinity relationship in the fjord. The system functioned as an  
48 automated mixing manifold that adjusted flow rates of warmed and chilled ambient seawater,  
49 with unmanipulated ambient seawater and freshwater delivered as a single source of mixed  
50 media to individual mesocosms. These conditions were maintained via continuously measured  
51 temperature and salinity in all 12 mesocosms (1 control and 3 treatments, all in triplicates) for 54  
52 days. System regulation was robust as median deviations from nominal conditions were  $< 0.15$   
53 for both temperature ( $^{\circ}\text{C}$ ) and salinity across the 3 replicates per treatment. Regulation further  
54 improved during a second deployment that mimicked three marine heatwave scenarios where a  
55 dynamic temperature regulation held median deviations to  $< 0.036^{\circ}\text{C}$  from the nominal value for  
56 all treatment conditions and replicates. This perturbation system has the potential to be

57 implemented across a wide range of conditions to test single or multi-stressor drivers (e.g.,  
58 increased temperature, freshening, high CO<sub>2</sub>) while maintaining natural variability. The  
59 automated and independent control for each experimental unit (if desired) provides a large  
60 breadth of versatility with respect to experimental design.

61

## 62 **1 Introduction**

63 The persistent burning of fossil fuels since the industrial revolution has radically increased  
64 atmospheric CO<sub>2</sub>. This has led to an enhanced greenhouse effect resulting in a multitude of  
65 changing climatic elements such as increasing sea surface temperature (Bindoff et al., 2019). In  
66 fjord systems, the confluence of increased fluvial inputs, glacier and permafrost meltwater,  
67 stratification and water mass intrusion, as well as increased sea surface temperatures can create  
68 periods of extreme physicochemical conditions for nearshore benthic and pelagic marine  
69 communities (Bhatia et al., 2013; Poloczanska et al., 2016; Divya and Krishnan, 2017; Bindoff et  
70 al., 2019). As ocean changes progress, the need to better understand the effects of combined  
71 stressors (e.g., increased temperature and freshening) on marine communities is essential to  
72 understand how community function and species richness will be affected while ecosystems  
73 adjust to these new environmental conditions (Kroeker et al., 2017; Wake, 2019; Orr et al.,  
74 2020). Several methodological approaches have been used to assess and characterize the  
75 response of organisms and communities to future ocean changes, such as *ex-situ*  
76 experimentation, the use of natural analogues (e.g., CO<sub>2</sub> vents), and space-for-time substitution  
77 (using spatial phenomena to model temporal changes) (Blois et al., 2013; Rastrick et al., 2018;  
78 Bass et al., 2021). These approaches, however, can be limited from testing the full range and  
79 dynamics of present and future environmental conditions. The use of *ex-situ* experimental

80 systems that manipulate multiple environmental conditions, such as temperature and salinity, can  
81 therefore provide a valuable tool to assess the response to multi-stressors in a future ocean.

82         The necessity of conducting multi-stressor experiments has become more pressing due to  
83 the increasing interactions of environmental drivers within dynamic systems under a changing  
84 climate (Kroeker et al., 2020). Nearshore regions can experience amplified modulations of  
85 temperature and salinity on short timescales (Evans et al., 2015; Hales et al., 2016; Fairchild and  
86 Hales, 2021). Such instances have been observed in sub-Arctic estuaries where water  
87 temperature at a depth of 10 m decreased by 1.5°C in < 10 h, and in temperate systems where the  
88 magnitude of salinity change driven by high precipitation displayed a decrease of 4 units in < 24  
89 h (Miller and Kelley, 2021; Poppeschi et al., 2021). Changes of this magnitude are particularly  
90 pertinent for Arctic fjords, where the variations in salinity from glacial meltwater can influence  
91 whether a system exhibits net heterotrophic or autotrophic characteristics (Sejr et al., 2022).

92         Recent advances in the ability to modulate several environmental parameters at once  
93 using *ex-situ* mesocosms have been made via the use of modular programmable systems (Wahl  
94 et al., 2015; Pansch and Hiebenthal, 2019). Such systems have demonstrated an ability to apply  
95 programmable environmental scenarios as a multifactorial design, or as a delta-change (offset)  
96 from ambient conditions that mimic the natural variability of an environment. The advantages of  
97 these types of automated systems lie in their ability to overcome the need for capturing and  
98 measuring abundant discrete measurements used to regulate experimental conditions, and  
99 transcend the logistical difficulties of implementing natural variability to experimental designs.  
100 In addition, these systems can reduce the need for constant human observation which may be  
101 required to program new regulatory operations or make rapid adjustments to experimentally  
102 manipulated conditions.

103 Here, we describe an autonomous salinity and temperature experimental perturbation  
104 mesocosm system (SalTExPreS) that has the ability to modify, and then regulate, salinity and  
105 temperature in real-time. The SalTExPreS can perform similar functions as the *ex-situ* mesocosm  
106 systems discussed above (i.e., Kiel-outdoor and -indoor benthocosms), such as applying  
107 programmable static or dynamic changes to temperature and salinity, or by replicating natural  
108 variability as an offset in real-time, but has the added capability of autonomous control for each  
109 experimental unit (e.g., chamber or mesocosm). In the initial deployment of the SalTExPreS, we  
110 applied a delta offset (i.e., offset from a measured control) to temperature and salinity as a  
111 fractional-factorial treatment design for a two-month long experiment in KongsFjorden,  
112 Svalbard, that exposed mixed kelp communities to future temperature, salinity, and irradiance.  
113 This study demonstrates the stability and flexibility of the SalTExPreS as an experimental tool to  
114 be utilized under extreme and dynamic conditions to test the effects of physicochemical multi-  
115 stressors on marine organisms and communities in the context of a multi-month experiment.

116

## 117 **2 Methods**

### 118 **2.1 Operational Concept of the Experimental System:**

119

120 The SalTExPreS simulates the drivers in a marine or freshwater system such as temperature,  
121 freshening, acidification, or hypoxia as either static or as temporally-variable modifications to a  
122 reference water source. This is accomplished by mixing manipulated source water, whether it is  
123 freshwater or warmed water, with ambient water through automatic flow valves that control the  
124 volume and rate of water delivered. This is regulated by the constant monitoring of the mixed  
125 water conditions in each mesocosm or chamber via a programmable feedback loop that transmits  
126 the opening or closing of the automatic flow valves. The automated ability of the SalTExPreS is

127 configured to respond to near instantaneous measurements (several reads per second) to achieve  
128 high frequency regulation of the manipulated drivers based on a measured *in-situ* or control  
129 reference. The programmable nominal conditions in each mesocosm are easily controllable  
130 through an intuitive user interface.

131

## 132 **2.2 Site Description and Experimental Design**

133 Kongsfjorden is a fjord system on the west coast of Svalbard (Norway) where the West  
134 Spitsbergen Current exchanges warm Atlantic water through sill channels based on differences in  
135 density gradients at the fjord mouth. Over the past two decades, a persistent influx of Atlantic  
136 water has resulted in the reduction of sea ice and the melting of marine-terminating glaciers  
137 causing enhanced freshwater and fluvial input (Luckman et al., 2015; Tverberg et al., 2019). The  
138 influx of freshwater is highest in summer and is accompanied by an important sediment loading  
139 with the potential to reduce the euphotic zone from 30 to 0.3 m depth (Svendsen et al., 2002).  
140 These climatic changes in the Kongsfjorden environment set a relevant context for the inaugural  
141 experiment of the SalTEXPreS. It was placed on a concrete platform situated ~ 12 m from the  
142 shoreline in Ny-Ålesund, which is located on southwestern shore of Kongsfjorden ~ 11 km from  
143 the fjord mouth.

144         The SalTEXPreS was utilized to implement three treatment scenarios in a fractional-  
145 factorial design to simulate expected future conditions in Kongsfjorden for a 54-d experiment  
146 that supervised the productivity, survival, and growth response of mixed kelp communities  
147 surveyed at 7 m (maximum depth of collection). The treatments were realized by multi-driver  
148 combinations of temperature, freshening, and irradiance, where treatments 1 and 2 differed in the  
149 magnitude of temperature increase, salinity decrease, and irradiance decrease (Table 1). Only

150 temperature was manipulated for treatment 3. The chosen treatment and salinity perturbations  
151 were applied as offset values from *in-situ* fjord conditions, which were measured at an  
152 underwater observatory fixed at 11 m depth and captured the natural variability of the fjord  
153 system. The applied temperature offsets used for this experiment reflected the projected SSP2-  
154 4.5 and SSP5-8.5 scenarios (Meredith et al., 2019; Overland et al., 2019; Table 1). The chosen  
155 decreases in salinity were based on correlations between *in-situ* temperature and salinity during  
156 summer 2020 in Kongsfjorden (Gattuso et al., 2023), weeks 22 to 35 (Appendix A1 and Fig.  
157 A1). These calculated delta salinity values were applied as offsets in treatments 1 and 2 (Table  
158 1). The third treatment scenario applied a temperature change of + 5.3°C as a way to decouple  
159 the multi-stressor system and evaluate a temperature only stress. The effect of turbidity for  
160 treatments 1 and 2 were simulated as a decrease in surface irradiance (i.e., ~ 25% and ~ 40%  
161 reduction from ambient irradiance at 7 m) by applying a combination of neutral light and spectral  
162 filters (Lee© Filters) placed as static fixtures over the top of the mesocosms. The response of  
163 these kelp community assemblages was determined in part by conducting weekly closed system  
164 incubations and assessing the growth and metabolism of the kelp in each mesocosm—details and  
165 results of this experiment are discussed elsewhere (Lebrun et al. *in review*; Miller et al., *in*  
166 *review*).

167

### 168 **2.3 Experimental System**

169

170 Water was pumped from Kongsfjorden at a 10 m depth (300 m offshore) using a submersible  
171 pump (NPS© Albatros F13T) that was tapped into an underwater intake pipe and that fed a  
172 header tank in the Kings Bay Marine Laboratory in Ny-Ålesund, Svalbard. To prevent clogging  
173 from sediment, the pump was situated at a 10 m depth ensuring a safe height above sediment

174 resuspension from the floor. Pumped ambient seawater from the header tank was then split into  
175 three sub-header tanks within the marine lab where ambient water was (1) left unchanged, (2)  
176 chilled to 0°C, or (3) warmed to 15°C. Each sub-header tank was plumbed to supply a maximum  
177 flow of 6 m<sup>3</sup> h<sup>-1</sup> for the ambient, 1 m<sup>3</sup> h<sup>-1</sup> for chilled, and 2 m<sup>3</sup> h<sup>-1</sup> of warmed water which  
178 required a pressure of 0.3 bars for each line to ensure consistent flow rates (Fig. 1). The three  
179 control mesocosms received a mix of chilled and ambient seawater in order to properly simulate  
180 *in-situ* temperatures. The three experimental treatments (nine mesocosms in total) received a mix  
181 of ambient, warmed, and freshwater for treatments 1 and 2, whereas treatment 3 received a mix  
182 of just ambient and warmed water (Fig 1). Freshwater was sourced from the tap which is fed by  
183 the Tvillingvann reservoir close to Ny-Ålesund. The total flow-through rate of each mesocosm  
184 was 0.5 m<sup>3</sup> h<sup>-1</sup> (i.e., each mesocosm turned over every 2 h) of post-mixed media delivered in an  
185 open cycle flow-through system, which was the necessary flow rate needed to maintain the target  
186 nominal values. Continuous flow was maintained throughout the experiment except for weekly 3  
187 h interruptions (to perform experiments on the community) where the flow to each mesocosm  
188 was shut off. In total, there were twelve circular mesocosms (3 treatments and 1 control, each  
189 with 3 replicates) with a mean diameter of 1.1 m and a volume of 1 m<sup>3</sup>, each equipped with a 12  
190 W wave pump (Sunsun© JVP-132), a temperature-conductivity probe (Aqualabo, PC4E), an  
191 optical oxygen sensor (Aqualabo, PODOC), and an Odyssey© light logger. Fiberglass insulation  
192 at the outside of each mesocosm reduced unintended changes in treatment water temperature.

193         Delivery of ambient, chilled, warmed and freshwater first ran through an automated  
194 mixing manifold that regulated the flow of each media type assuring that proper volumetric  
195 proportions passed through the regulator valves to achieve target conditions (Fig. 1). Each  
196 source-water flow line was regulated by an automated 2-way mixing valve (including the



197 incoming freshwater line) which then passed through a 3-way mixing valve that was assigned to  
198 each mesocosm (12 in total, Fig. 1). This style of regulation ensured that the proper proportions  
199 of manipulated media and ambient water were mixed to achieve nominal conditions. Any  
200 temperature variation induced by mixing freshwater was immediately compensated for by  
201 regulating the flow of the warm water line. Details regarding the programmed regulation are  
202 discussed further in the appendix (Section A2). The mixed media then passed through a flow  
203 meter which measured the flow rate to each mesocosm. A hand-crank regulating valve was  
204 placed directly after the flow meter and was used for making minor adjustments and controlling  
205 the overall flow. Measurements by the pressure sensors, the status of open position for the  
206 regulator valves, and flow rates were logged every minute and displayed on the user interface  
207 (Fig. A3).

208

## 209 **2.4 Nominal Regulation**

210

211 Nominal temperature conditions of + 3.3, 5.3, and 5.3°C applied to treatments 1, 2, and 3,  
212 respectively, were offsets from the nominal control temperature. The nominal temperature of the  
213 control was updated hourly and programmed to replicate the measured *in-situ* conditions in the  
214 fjord logged by the AWIPEV (Alfred Wegener Institute and Institute Paul Emile Victor)  
215 FerryBox part of the COSYNA underwater observatory (<https://dashboard.awi.de/>) situated at a  
216 depth of 11 m. Each treatment condition (temperature and salinity offset) was set by manually  
217 programming the nominal value of temperature in the software interface (see appendix A3). The  
218 salinity offset was coupled to the nominal temperature via the correlation described in appendix  
219 A1. The measured temperature and salinity observations from inside each mesocosm were  
220 recorded multiple times per minute and used to continuously monitor the regulation of the

221 conditions inside each mesocosm. This data transmission was used to program the software  
222 controller that performed the automated regulation of mixed media (for details see appendix A2).

## 223 224 **2.5 Software**

225 The software application used for the control of the SalTExPreS was developed using Visual  
226 Studio Community (2019 edition) with the vMicro extension and Arduino 1.8.13. The program  
227 application has a user-friendly interface designed to allow real-time monitoring and  
228 parameterization of regulation processes (Fig. A3). The main window displays each mesocosm  
229 condition (the parameters measured by a sensor), their piping connections, a connection status  
230 for each Programmable Logic Controller (PLC) informing on proper communication, date and  
231 time of the last received communication packet from the Head PLC, and the status of the  
232 experiment (e.g., started or stopped). The interface also displays the valve opening percentage  
233 along with the nominal pressure and the actual measured value for each main source-water inlet.  
234 In addition, the *in-situ* data (temperature and salinity) received from the FerryBox is displayed  
235 with the time and date of the last logged value utilized to program the real-time nominal value of  
236 the control. Sensor readings of flow rate ( $\text{L min}^{-1}$ ),  $\text{O}_2$  saturation (%), salinity, and temperature  
237 ( $^{\circ}\text{C}$ ) are shown for each mesocosm in conjunction with the treatment nominal values (i.e.,  
238 temperature, and salinity when relevant). All measured data are stored through the server  
239 connection to the cloud, however, there is a backup microSD card on the Head PLC that logs  
240 data from all mesocosms every 5 sec. If communication fails between the Head PLC and the  
241 interfaced computer, data will not be retrieved by the PC during the communication break but  
242 will be retained by the microSD card.

## 243 244 **3 Results**

245  
246  
247  
248  
249  
250  
251  
252  
253  
254  
255  
256  
257  
258  
259  
260  
261  
262  
263  
264  
265  
266  
267  
268  
269  
270  
271

### 3.1 Regulation of the Control

The control was able to simulate the ambient fjord temperature well over the experimental period where the average value across the 3 replicates deviated  $< 0.3^{\circ}\text{C}$  (Table 2, Fig. 2). The overall quality of the regulation was achieved by the ability of the system to interpret and respond to the measured data from the FerryBox (or to follow a manually programmed nominal value when communication with the FerryBox was interrupted). During the experiment, the FerryBox went intermittently offline 24% of the time, ceasing transmission of real-time data that resulted in a break of communication to the PLCs. This somewhat frequent break in communication resulted in an average nominal deviation that was nearly double for the control compared to the treatment conditions (Table 2). The ability to manually program a new nominal value when communication breaks occurred ensured that the control remained robustly regulated. Over the entire period of the SalTExPreS deployment, the mean temperature of the control increased from  $\sim 4$  to  $6.5^{\circ}\text{C}$  from early July to the end of August (Fig. 3a). The coldest mean temperature of the control occurred when a backup pump situated at 90 m depth in the fjord was used from 2021-07-14  $\sim 21:00$  UTC until 2021-07-26 13:49 UTC while the original pump at 10 m depth was repaired. During this period, the control was  $\sim 1.0 - 1.5^{\circ}\text{C}$  cooler than the temperature measured by the FerryBox (Figs. 2, 3). Since a warmed seawater inlet was not supplied to the control, the temperature of the control remained cooler than the measured ambient conditions at the FerryBox. Despite the cooler temperature for the control, regulation of flow rates, mesocosm turnover time, and variability across the control replicates was well maintained by the system.

### 1.2 Temperature and Salinity Regulation

272  
273 The regulation of temperature and salinity in the different treatment conditions (Trts. 1 – 3) was  
274 maintained by the SalTExPreS for the full planned duration of 54 days (2021-07-03 to 2021-08-  
275 26). For the first 6 days of the SalTExPreS experiment, the treatment conditions were held at the  
276 control (i.e., no applied offset from the control) before the stepwise increase in temperature  
277 began. On 2021-07-10 12:00 UTC a temperature offset of  $0.55^{\circ}\text{C d}^{-1}$  was programmed for  
278 treatment 1 while treatment 2 and 3 were programmed to increase by  $0.88^{\circ}\text{C d}^{-1}$  (Figs. 2, 3). The  
279 final nominal temperature above the control was reached on 2021-07-15 21:00 UTC. The system  
280 needed 4 h to achieve the new temperature conditions (i.e., homogenize the mesocosm to a  
281  $0.88^{\circ}\text{C}$  increase). A manual override was applied to the salinity regulation for treatments 1 and 2  
282 which resulted in the system achieving the final salinity offset value upon the initial temperature  
283 increase (Fig. 3b, 4). This was done to ensure the maintenance of salinity regulation as the  
284 temperature offsets were applied relative to the control, which was receiving fjord water pumped  
285 from 90 m and was colder than the measured *in-situ* conditions. It took the system 4 h to achieve  
286 the salinity offset for treatment 2 adjusting the value from  $\sim 34$  to 29.8 (Fig. 3b, 4).

287 The precision of the temperature and salinity regulation across all treatment conditions  
288 was well maintained as the mean difference between the measured value and the nominal value  
289 was  $< 0.2^{\circ}\text{C}$  and  $< 0.36$  for salinity across the entire deployment (Table 2). The mean deviations  
290 observed across treatments did not appear to correlate to the degree of offset. Thus, treatment 3  
291 showed the highest precision for temperature regulation, while salinity regulation was the most  
292 robust for treatment 2 compared to treatment 1 (Table 2). During several instances when  
293 communication was interrupted between the FerryBox and the Head PLC, the SalTExPreS  
294 retained the last measured value at the FerryBox as a contingency protocol. This aided in the  
295 ability of the system to maintain a high degree of regulation throughout the entire deployment.

296 The largest deviation from the nominal value for all treatment conditions occurred during the  
297 single instance in which the last read value from the FerryBox was not retained: this occurred on  
298 2021-08-24 04:47 UTC (Fig. 4). Communication was quickly restored after this incident by  
299 cycling the program code, and the average deviation of temperature ( $^{\circ}\text{C}$ ) and salinity for  
300 treatment 1 for the remainder of the deployment was  $< 0.16$ , and  $< 0.25$  for treatment 2.

301 When adequate flow rates were maintained, the SalTExPreS was able to simultaneously  
302 regulate 12 mesocosms at 4 different conditions to deviations in temperature and salinity that  
303 were  $< 0.5^{\circ}\text{C}$  or 0.5 in salinity from the nominal value  $\geq 80\%$  and  $\geq 70\%$  of the time,  
304 respectively (Fig. 5). Due to an erroneous nominal value for the control during the 90 m pump  
305 usage, these times were excluded. If warm water could have been mixed with the ambient water  
306 feeding the control mesocosms, then a proper nominal value could have been maintained. Over  
307 the full duration of the experiment, effective regulation from the nominal temperature and  
308 salinity values were kept to  $< 1$  for all mesocosms 89% of the time for temperature ( $^{\circ}\text{C}$ ), and  
309 80% for the salinity (excluding the 1<sup>st</sup> replicate for treatment 2).

310

## 311 **Discussion**

312

313 The first application of the fully autonomous SalTExPreS demonstrated the capacity of the  
314 system to successfully manipulate temperature and salinity as an offset value from the control,  
315 thus maintaining, natural, *in-situ* variability for 4 different conditions simultaneously. We  
316 utilized this deployment to test the effects of climate change drivers on Arctic kelp communities  
317 recognizing the feasibility of the system to perform *ex-situ* experiments on organisms or whole  
318 communities (Miller et al., *in review*). The versatility of the system not only allows for the  
319 manipulation of temperature and salinity, but can incorporate other factors such as  $\text{CO}_2$  or

320 hypoxia (Gazeau et al., *in prep*). While this experiment used a control offset approach to produce  
321 treatment conditions, programmable parametrization of various treatment combinations can be  
322 applied depending on the question and design of the experiment. The automated component of  
323 the system reduced the logistical hurdles that can arise when performing high precision  
324 replication and regulation of experimental conditions that track real-time system variability.  
325 While the use of such a system can reduce user oversight and limitations, there is still a need for  
326 diligent operation.

327         Since the initial experiment, we have implemented a number of changes to improve the  
328 performance of the system which have been realized during a second experiment in the summer  
329 of 2022 (Fig. 6). In this experiment, the SalTExPreS was integrated to function with a deployable  
330 heat pump to simulate multiple scenarios of marine heatwave patterns over a nearly month-long  
331 experiment. In this instance, temperature regulation was vastly improved as a result of the  
332 programmable modifications made since the initial experiment. During this second experiment,  
333 the SalTExPreS mimicked 3 marine heatwave scenarios where a dynamic temperature regulation  
334 kept deviations in the 9 different mesocosms at  $< 0.5^{\circ}\text{C}$  for 94% of the time. This was an  
335 improvement to the % time of temperature regulation by  $\sim 15\%$  compared to the first  
336 experiment. During the first experiment, inconsistent flow rates and communication errors  
337 between the FerryBox and the Head PLC were the primary causes of larger deviations ( $> 2.0$   
338 salinity or  $^{\circ}\text{C}$ ) from nominal values. For example, flow rates of  $< 2 \text{ L min}^{-1}$  accounted for  $\sim 20\%$   
339 of the large deviations in temperature and salinity regulation. Simple software modifications  
340 such as ‘pop-up’ alert windows that warned when a lapse in communication with the FerryBox  
341 occurred (e.g., FerryBox stopped logging), and the addition of contingency coding instructions  
342 (i.e., fail-safe instructions) ensuring that the last received *in-situ* data were maintained solved

343 most of the issues. Communication errors were easily remedied by cycling the power on a PLC,  
344 which is why pop-up alerts were an improvement to the operation. Other extraneous  
345 circumstances that could impact flow rates, such as pump failure and clogging of the seawater  
346 intake ports, are issues that need to be addressed whenever the SalTExPreS is used. However,  
347 these are very manageable situations which can be easily mitigated by an operator.

348         The novelty of the SalTExPreS lies in its ability to independently regulate experimental  
349 conditions in a single experimental chamber (e.g., mesocosm). The operational data produced  
350 from this deployment are reliable, easily quantifiable, and provide the highest degree of  
351 monitoring frequency for every applied experimental condition. This study has demonstrated the  
352 system's ability to replicate dynamic nearshore environments where temperature and salinity can  
353 vary at high frequency (e.g., tidally). The system's additional capacity to mimic future scenarios  
354 by applying an amplitude offset to the natural dynamics of *in-situ* conditions is an added feature  
355 for conducting manipulative experiments. Wahl et al. (2015) described a system with a similar  
356 capability, but regulated treatment conditions by monitoring source water and adjusting that  
357 media before it was delivered to each experimental chamber. The SalTExPreS differs in that it  
358 measures the conditions inside each experimental chamber (i.e., mesocosm) and regulates them  
359 independently based on per second measurements. This provides the flexibility to individually  
360 modulate each experimental chamber providing a broad range of versatility. The lack of  
361 infrastructure needed to set up the SalTExPreS makes it easy to deploy and transport. As long as  
362 there is a sufficient supply of ambient water and manipulated media, there is little limit to the  
363 versatility of automated control for each mesocosm. Many research endeavors and future  
364 implementations by the SalTExPreS have the potential to conduct a large range of experimental  
365 settings that pertain to environmental perturbations associated with climate change or other

366 anthropogenic forcings. The operation of such a system in extreme environmental conditions has  
367 shown the durability of the manifold to endure an adverse Arctic summer and still respond  
368 without mechanical failures. With proper operation and user proficiency, this proves to be a  
369 highly sophisticated and powerful tool to be utilized for marine and aquatic perturbation  
370 experiments.

371

### 372 **Acknowledgements**

373 This study is part of the FACE-IT Project (The Future of Arctic Coastal Ecosystems –  
374 Identifying Transitions in Fjord Systems and Adjacent Coastal Areas). The authors thank Jens  
375 Terhaar for helping with temperature projection data, Philipp Fischer for access to the AWIPEV  
376 data as well as AWIPEV and Kings Bay staff for helping with logistical details, shipping, and  
377 access to the marine lab facilities.

378

### 379 **Author contributions**

380 C.M. and F.G. conceptualized the frame of the paper while F.G, S.C, and P.U. designed the  
381 experimental system. P.U. programmed the software. C.M. wrote the manuscript, performed the  
382 data analysis, and constructed the figures and tables while P.U. designed schematic figures. All  
383 authors participated in the operation of the system and have, thus, commented, and edited during  
384 writing.

385

### 386 **Data availability**

387 The dataset presented in this paper can be found here:

388 <https://doi.pangaea.de/10.1594/PANGAEA.961785>.



389 **Financial support**

390 This study was conducted in the frame of the project FACE-IT (The Future of Arctic Coastal  
391 Ecosystems – Identifying Transitions in Fjord Systems and Adjacent Coastal Areas). FACE-IT  
392 has received funding from the European Union’s Horizon 2020 research and innovation  
393 programme under grant agreement No 869154. Logistical and financial support was provided by  
394 IPEV, The French Polar Institute and the Foundation Prince Albert 2 of Monaco (project: 3051,  
395 <http://fpa2.org>).

396

397 **Competing interest**

398 The authors declare no competing interests exist.

399 **References**

- 400 Bass, A., Wernberg, T., Thomsen, M., and Smale, D.: Another Decade of Marine Climate  
401 Change Experiments: Trends, Progress and Knowledge Gaps, *Frontiers in Marine Science*, 8,  
402 2021.
- 403 Bhatia, M. P., Kujawinski, E. B., Das, S. B., Breier, C. F., Henderson, P. B., and Charette, M. A.:  
404 Greenland meltwater as a significant and potentially bioavailable source of iron to the ocean,  
405 *Nature Geosci*, 6, 274–278, <https://doi.org/10.1038/ngeo1746>, 2013.
- 406 Bindoff, N. L., Cheung, W. W. L., Kairo, J. G., Arístegui, J., Guinder, V. A., Hallberg, R.,  
407 Hilmi, N., Jiao, N., Karim, M. S., Levin, L., O’Donoghue, S., Purca Cuicapusa, S. R., Rinkevich,  
408 B., Suga, T., Tagliabue, A., and Williamson, P.: Chapter 5: Changing Ocean, Marine  
409 Ecosystems, and Dependent Communities — Special Report on the Ocean and Cryosphere in a  
410 Changing Climate, 2019.
- 411 Blois, J. L., Williams, J. W., Fitzpatrick, M. C., Jackson, S. T., and Ferrier, S.: Space can  
412 substitute for time in predicting climate-change effects on biodiversity, *Proc Natl Acad Sci U S*  
413 *A*, 110, 9374–9379, <https://doi.org/10.1073/pnas.1220228110>, 2013.
- 414 Divya, D. T. and Krishnan, K. p.: Recent variability in the Atlantic water intrusion and water  
415 masses in Kongsfjorden, an Arctic fjord, *Polar Science*, 11, 30–41,  
416 <https://doi.org/10.1016/j.polar.2016.11.004>, 2017.
- 417 Evans, W., Mathis, J. T., Ramsay, J., and Hetrick, J.: On the frontline: Tracking ocean  
418 acidification in an Alaskan shellfish hatchery, *PLOS ONE*, 10, e0130384,  
419 <https://doi.org/10.1371/journal.pone.0130384>, 2015.

420 Fairchild, W. and Hales, B.: High-Resolution Carbonate System Dynamics of Netarts Bay, OR  
421 From 2014 to 2019, *Frontiers in Marine Science*, 7, 2021.

422 Gattuso, J.-P., Alliouane, S., and Fischer, P.: High-frequency, year-round time series of the  
423 carbonate chemistry in a high-Arctic fjord (Svalbard), *Earth System Science Data*, 15, 2809–  
424 2825, <https://doi.org/10.5194/essd-15-2809-2023>, 2023.

425 Hales, B., Suhrbier, A., Waldbusser, G. G., Feely, R. A., and Newton, J. A.: The Carbonate  
426 Chemistry of the “Fattening Line,” Willapa Bay, 2011–2014, *Estuaries and Coasts*, 1–14,  
427 <https://doi.org/10.1007/s12237-016-0136-7>, 2016.

428 Kroeker, K. J., Kordas, R. L., and Harley, C. D. G.: Embracing interactions in ocean  
429 acidification research: confronting multiple stressor scenarios and context dependence, *Biology*  
430 *Letters*, 13, 20160802, <https://doi.org/10.1098/rsbl.2016.0802>, 2017.

431 Kroeker, K. J., Bell, L. E., Donham, E. M., Hoshijima, U., Lummis, S., Toy, J. A., and Willis-  
432 Norton, E.: Ecological change in dynamic environments: Accounting for temporal environmental  
433 variability in studies of ocean change biology, *Global Change Biology*, 26, 54–67,  
434 <https://doi.org/10.1111/gcb.14868>, 2020.

435 Lebrun, A., Miller, C. A., Meynadier, M., Comeau, S., Urrutti, P., Alliouane, S., Schlegel, R.,  
436 Gattuso, J.-P., and Gazeau, F.: Multifactorial effects of warming, low irradiance, and low salinity  
437 on Arctic kelps, *EGU sphere* [preprint], <https://doi.org/10.5194/egusphere-2023-1875>, *in review*.  
438

439 Luckman, A., Benn, D. I., Cottier, F., Bevan, S., Nilsen, F., and Inall, M.: Calving rates at  
440 tidewater glaciers vary strongly with ocean temperature, *Nat Commun*, 6, 8566,  
441 <https://doi.org/10.1038/ncomms9566>, 2015.

442 Meredith, M., Sommerkon, M., Cassotta, S., Derksen, C., Ekaykin, A., Hollowed, A., Kofinas,  
443 G., Mackintosh, A., Melbourne-Thomas, J., Muelbert, M. M. C., Ottersen, G., Ptitchard, H., and  
444 Schuur, E. A. G.: Chapter 3: Polar regions — Special Report on the Ocean and Cryosphere in a  
445 Changing Climate, IPCC, 2019.

446 Miller, C., Gazeau, F., Lebrun, A., Gattuso, J.-P., Alliouane, S., Urrutti, P., Schlegel, R., and  
447 Comeau, S.: Productivity of Mixed Kelp Communities in an Arctic Fjord Exhibit Tolerance to a  
448 Future Climate, <https://doi.org/10.2139/ssrn.4563719>, *in review*.

449 Miller, C. A., Urrutti, P., Gattuso, J.-P., Comeau, S., Lebrun, A., Alliouane, S., Schlegel, R., and  
450 Gazeau, F.: Measurements of An Autonomous Flow through Salinity and Temperature  
451 Perturbation Mesocosm System for a Multi-stressor Experiment,  
452 <https://doi.org/10.1594/PANGAEA.961785>, 2023.  
453

454 Miller, C. A. and Kelley, A. L.: Seasonality and biological forcing modify the diel frequency of  
455 nearshore pH extremes in a subarctic Alaskan estuary, *Limnology and Oceanography*, 66, 1475–  
456 1491, <https://doi.org/10.1002/lno.11698>, 2021.

457 Orr, J. A., Vinebrooke, R. D., Jackson, M. C., Kroeker, K. J., Kordas, R. L., Mantyka-Pringle,  
458 C., Van den Brink, P. J., De Laender, F., Stoks, R., Holmstrup, M., Matthaei, C. D., Monk, W.

459 A., Penk, M. R., Leuzinger, S., Schäfer, R. B., and Piggott, J. J.: Towards a unified study of  
460 multiple stressors: divisions and common goals across research disciplines, *Proceedings of the*  
461 *Royal Society B: Biological Sciences*, 287, 20200421, <https://doi.org/10.1098/rspb.2020.0421>,  
462 2020.

463 Overland, J., Dunlea, E., Box, J. E., Corell, R., Forsius, M., Kattsov, V., Olsen, M. S., Pawlak, J.,  
464 Reiersen, L.-O., and Wang, M.: The urgency of Arctic change, *Polar Science*, 21, 6–13,  
465 <https://doi.org/10.1016/j.polar.2018.11.008>, 2019.

466 Pansch, C. and Hiebenthal, C.: A new mesocosm system to study the effects of environmental  
467 variability on marine species and communities, *Limnology and Oceanography: Methods*, 17,  
468 145–162, <https://doi.org/10.1002/lom3.10306>, 2019.

469 Poloczanska, E. S., Burrows, M. T., Brown, C. J., García Molinos, J., Halpern, B. S., Hoegh-  
470 Guldberg, O., Kappel, C. V., Moore, P. J., Richardson, A. J., Schoeman, D. S., and Sydeman, W.  
471 J.: Responses of Marine Organisms to Climate Change across Oceans, *Frontiers in Marine*  
472 *Science*, 3, 2016.

473 Poppeschi, C., Charria, G., Goberville, E., Rimmelin-Maury, P., Barrier, N., Petton, S.,  
474 Unterberger, M., Grossteffan, E., Repecaud, M., Quémener, L., Theetten, S., Le Roux, J.-F., and  
475 Tréguer, P.: Unraveling Salinity Extreme Events in Coastal Environments: A Winter Focus on  
476 the Bay of Brest, *Frontiers in Marine Science*, 8, 2021.

477 Rastrick, S. S. P., Graham, H., Azetsu-Scott, K., Calosi, P., Chierici, M., Fransson, A., Hop, H.,  
478 Hall-Spencer, J., Milazzo, M., Thor, P., and Kutti, T.: Using natural analogues to investigate the  
479 effects of climate change and ocean acidification on Northern ecosystems, *ICES Journal of*  
480 *Marine Science*, 75, 2299–2311, <https://doi.org/10.1093/icesjms/fsy128>, 2018.

481 Sejr, M. K., Bruhn, A., Dalsgaard, T., Juul-Pedersen, T., Stedmon, C. A., Blicher, M., Meire, L.,  
482 Mankoff, K. D., and Thyrring, J.: Glacial meltwater determines the balance between autotrophic  
483 and heterotrophic processes in a Greenland fjord, *Proceedings of the National Academy of*  
484 *Sciences*, 119, e2207024119, <https://doi.org/10.1073/pnas.2207024119>, 2022.

485 Svendsen, H., Beszczynska-Møller, A., Hagen, J. O., Lefauconnier, B., Tverberg, V., Gerland,  
486 S., Børre Ørbæk, J., Bischof, K., Papucci, C., Zajaczkowski, M., Azzolini, R., Bruland, O., and  
487 Wiencke, C.: The physical environment of Kongsfjorden–Krossfjorden, an Arctic fjord system in  
488 Svalbard, *Polar Research*, 21, 133–166, <https://doi.org/10.3402/polar.v21i1.6479>, 2002.

489 Tverberg, V., Skogseth, R., Cottier, F., Sundfjord, A., Walczowski, W., Inall, M. E., Falck, E.,  
490 Pavlova, O., and Nilsen, F.: The Kongsfjorden Transect: Seasonal and Inter-annual Variability in  
491 Hydrography, in: *The Ecosystem of Kongsfjorden, Svalbard*, edited by: Hop, H. and Wiencke,  
492 C., Springer International Publishing, Cham, 49–104, [https://doi.org/10.1007/978-3-319-46425-](https://doi.org/10.1007/978-3-319-46425-1_3)  
493 [1\\_3](https://doi.org/10.1007/978-3-319-46425-1_3), 2019.

494 Wahl, M., Buchholz, B., Winde, V., Golomb, D., Guy-Haim, T., Müller, J., Rilov, G., Scotti, M.,  
495 and Böttcher, M. E.: A mesocosm concept for the simulation of near-natural shallow underwater  
496 climates: The Kiel Outdoor Benthocosms (KOB), *Limnology and Oceanography: Methods*, 13,  
497 651–663, <https://doi.org/10.1002/lom3.10055>, 2015.

498 Wake, B.: Experimenting with multistressors, *Nat. Clim. Chang.*, 9, 357–357,  
499 <https://doi.org/10.1038/s41558-019-0475-z>, 2019.

500 Ziegler, J. G. and Nichols, N. B.: Optimum Settings for Automatic Controllers, *Transactions of*  
501 *the American Society of Mechanical Engineers*, 64, 759–765, <https://doi.org/10.1115/1.4019264>,  
502 1943.

503

504

505

506

507

508

509

510

511

512

513

514

515

516

517

518

519

520

521

522

523 **Tables**

524 **Table 1.** Experimental treatment conditions with corresponding offsets (as compared to the  
 525 control) for temperature (°C), salinity and photosynthetically active radiation (PAR; expressed as  
 526 a percentage). See section A1 and figure A1 for a full description of the temperature-salinity  
 527 relationship used to calculate salinity offsets.

<i>Treatment</i>	<i>Temperature</i>	<i>Salinity</i>	<i>PAR</i>
1	+ 3.3 °C	- 2.5 – 3.0 - $S = 0.546 * T + 0.490$	- 25% PAR
2	+ 5.3 °C	- 5.0 – 5.5 - $S = 0.877 * T + 0.089$	- 40% PAR
3	+ 5.3 °C	Ambient	Ambient

528

529

530

531

532

533

534

535

536

537

538

539

540

541

542 **Table 2.** Absolute mean difference between measured temperature ( $T_{\text{meas}}$ ; °C) and salinity ( $S_{\text{meas}}$ )  
543 values against nominal values ( $T_{\text{nominal}}$  and  $S_{\text{nominal}}$ ) plus or minus the corresponding standard  
544 deviation, in each mesocosm during the experimental period. A weighted average was used for  
545 treatments 1 – 3 to account for the initial 5-day incremental increase. Triplicate mesocosms per  
546 condition are expressed as a, b and c. Water mixture indicates the types of media supplied to  
547 each treatment, denoted with an ‘x’.

<i>Treatment</i>	<i>Mean diff</i>		<i>Water mixture</i>			
	<i>Abs(<math>T_{\text{meas}} - T_{\text{nominal}}</math>)</i>	<i>Abs(<math>S_{\text{meas}} - S_{\text{nominal}}</math>)</i>	<i>Cold</i>	<i>Ambient</i>	<i>Warm</i>	<i>Fresh</i>
<i>Control a</i>	0.275 ± 0.39	–	x	x		
<i>Control b</i>	0.291 ± 0.36	–	x	x		
<i>Control c</i>	0.223 ± 0.36	–	x	x		
<i>Treatment 1a</i>	0.126 ± 0.31	0.116 ± 0.31		x	x	x
<i>Treatment 1b</i>	0.142 ± 0.29	0.148 ± 0.22		x	x	x
<i>Treatment 1c</i>	0.145 ± 0.33	0.171 ± 0.33		x	x	x
<i>Treatment 2a</i>	0.111 ± 0.29	0.357 ± 0.74		x	x	x
<i>Treatment 2b</i>	0.133 ± 0.29	0.149 ± 0.26		x	x	x
<i>Treatment 2c</i>	0.196 ± 0.38	0.128 ± 0.25		x	x	x
<i>Treatment 3a</i>	0.109 ± 0.27	–		x	x	
<i>Treatment 3b</i>	0.112 ± 0.27	–		x	x	
<i>Treatment 3c</i>	0.106 ± 0.28	–		x	x	

548

549

550

551

552

553

554

555

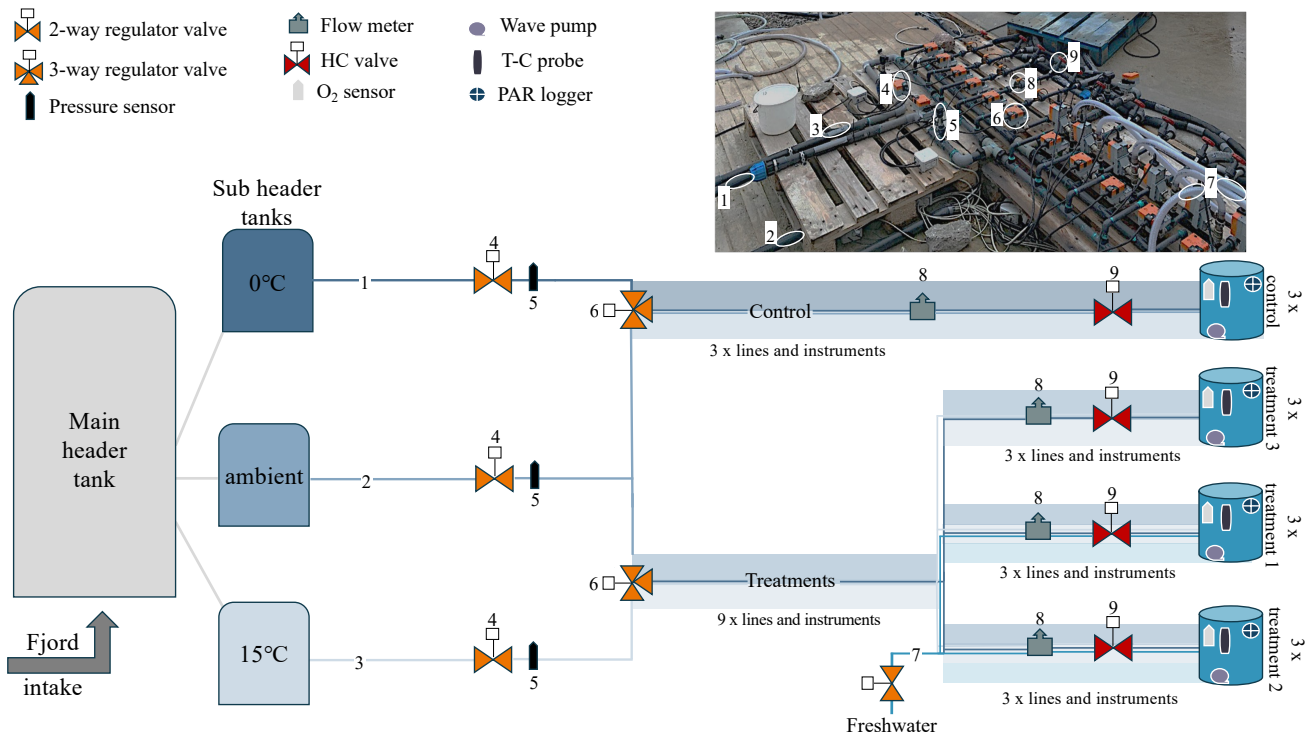
556

557

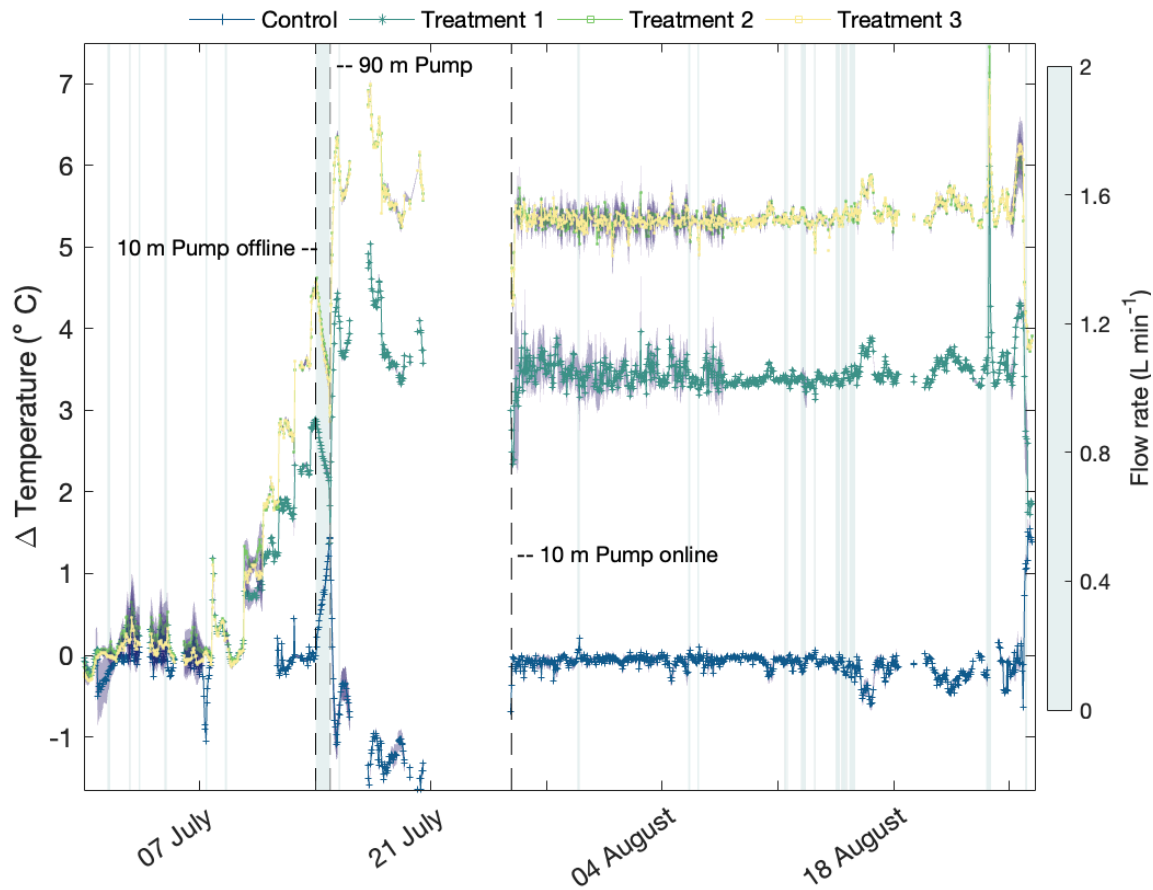
558

559

560 **Figures**



562 **Figure 1.** Piping schematic of the SaITeXPreS which includes the mixing and regulation  
 563 manifold. Items 1 – 3 depict the main seawater inlets from the chilled, ambient, and warmed sub-  
 564 header tanks located in the Kings Bay Marine Laboratory. Seawater from each sub-header tank  
 565 moves through a 2-way regulator (4) valve followed by a pressure sensor (5) before splitting into  
 566 individual lines that lead to all 12 3-way regulator valves (6), each assigned to a single  
 567 mesocosm. For treatments 1 and 2, the freshwater inlet (clear tube; item 7) passes through a 2-  
 568 way regulator valve before mixing with the ambient and warmed seawater lines. Flow rates are  
 569 then measured (8) post-mixing, and final flow rates are set using a hand-crank (HC) red valve  
 570 (9). The shaded regions in the schematic indicate that mixed media lines and instruments occur  
 571 3x or 9x times. T-C probe is the temperature-conductivity probe and the PAR logger measures  
 572 the photosynthetically active radiation. Photos of mesocosms and the sensors inside can be found  
 573 in the appendix (Fig. A6). Table A1 provides the parts list for the items shown in this figure.



575

576 **Figure 2.** The hourly mean (across triplicated mesocosms) temperature offsets of all applied  
 577 conditions. For control mesocosms (in blue), offsets were calculated against *in-situ*  
 578 measurements (FerryBox). For the three experimental treatments (dark green, light green, and  
 579 yellow for treatments 1, 2 and 3, respectively), offsets were estimated against the mean control  
 580 values. The purple shaded region around the mean is the standard deviation. The heatmap  
 581 isoclines (blue-grey shaded regions) are instances when flow rates were  $\leq 2 \text{ L min}^{-1}$  (threshold to  
 582 avoid large deviations  $> 2.0$  salinity or  $^{\circ}\text{C}$ ). Dashed black lines indicate periods when the pump  
 583 at 10 m depth and 90 m depth were used to feed the sub-header tanks. The time presented is the  
 584 duration of the experimental deployment.

585



586



587

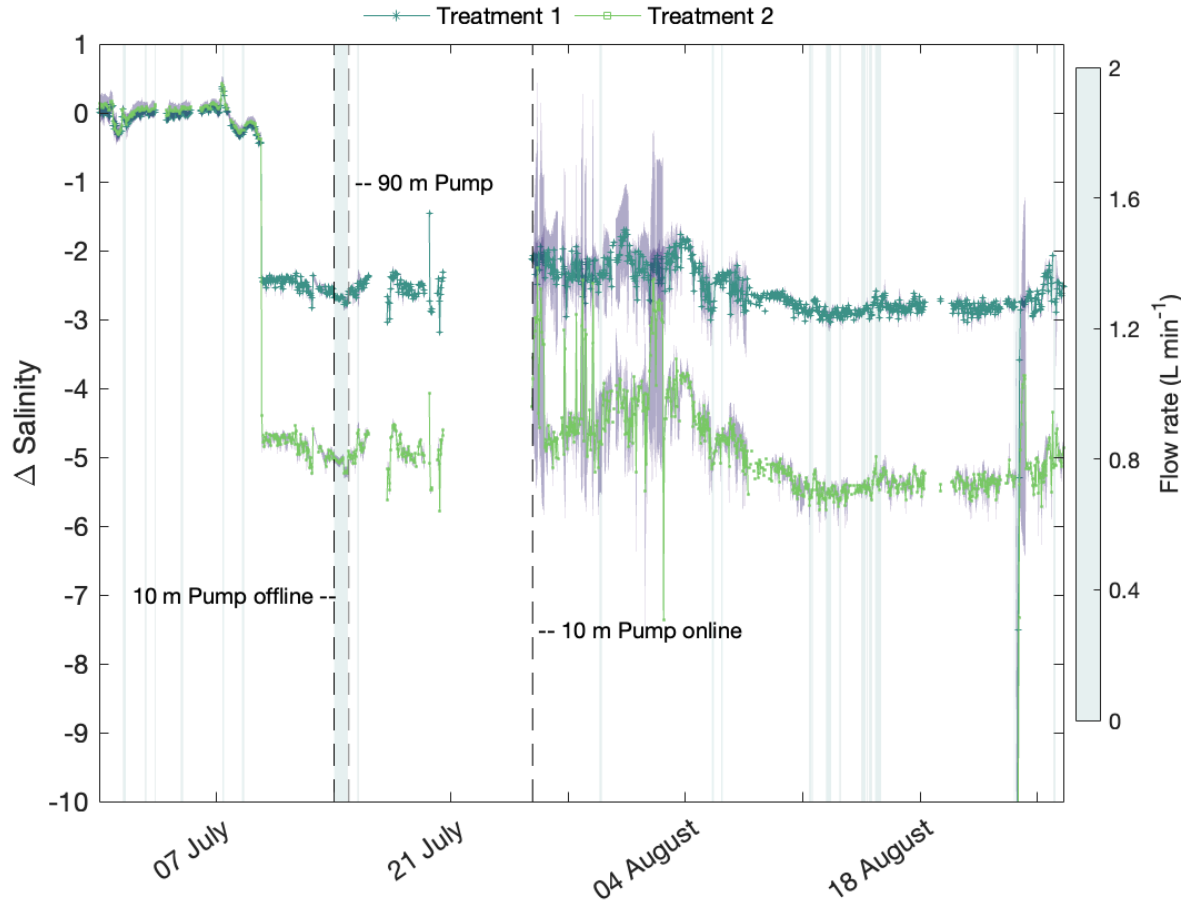
588 **Figure 3.** Mean (across triplicated mesocosms) temperature (°C; **a**) and salinity (**b**) values  
589 measured every minute over a 60 d period (including 6 day period before the start of the  
590 experiment) for the control (blue), and for treatments 1 – 3 (dark green, light green, and yellow,  
591 respectively).

592

593

594

595



596

597 **Figure 4.** The hourly mean (across triplicated mesocosms) salinity offsets for the experimental  
 598 period. Dark green is treatment 1 and light green is treatment 2. The purple shaded region around  
 599 the mean is the standard deviation and the heatmap isoclines (blue shaded regions) are the  
 600 instances when flow rates  $\leq 2 \text{ L min}^{-1}$ . Dashed black lines indicate periods when the pump at 10  
 601 m depth and 90 m depth were used to feed the sub-header tanks.

602

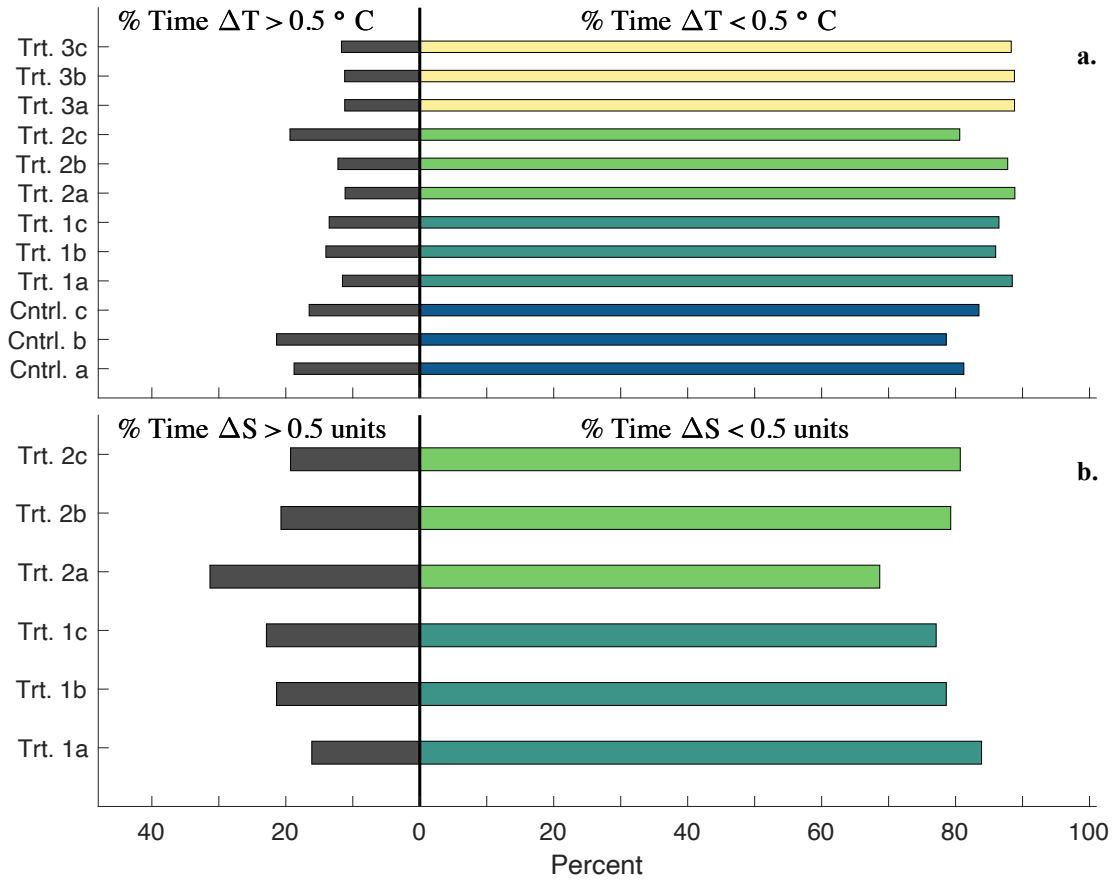
603

604

605

606

607



608

609

**Figure 5.** Percent time each mesocosm experienced a deviation > (black bars) or < (colored

610

bars) 0.5°C (ΔT; **a**) or 0.5 in salinity (ΔS; **b**) when flow rates were above 2 L min<sup>-1</sup>. Cntrl. and

611

Trt. abbreviations are the control and treatments, respectively. This excludes the period when

612

using the 90 m pump (12 d), but accounts for 42 days out of the 54-day experiment. Bar color

613

indicates different treatment groups, as shown on the y-axes.

614

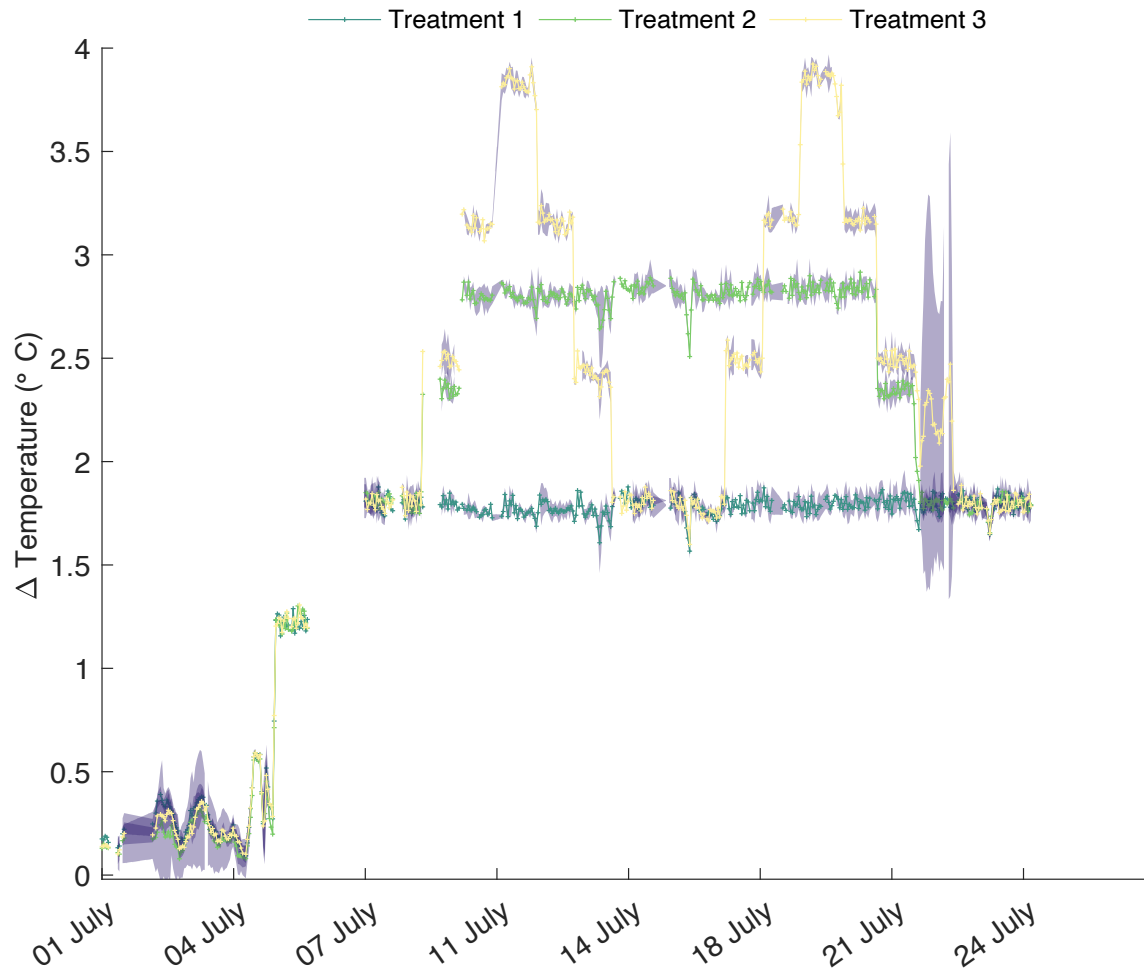
615

616

617

618

619



620

621 **Figure 6.** The hourly mean temperature offsets ( $\Delta$  Temperature) during the 2<sup>nd</sup> deployment of  
 622 SalTExPreS in the summer of 2022 in Tromsø (Norway) performing a variation of heatwave  
 623 scenarios with three experimental treatments 1 – 3. Treatment 1 is a constant high temperature (+  
 624 1.76°C), treatment 2 is a low frequency (1 heatwave) and medium magnitude offset (+ 2.81°C),  
 625 while treatment 3 is a high frequency (2 heatwaves) and magnitude offset (+ 3.86°C). The purple  
 626 shaded region around the mean is the standard deviation.

627

628

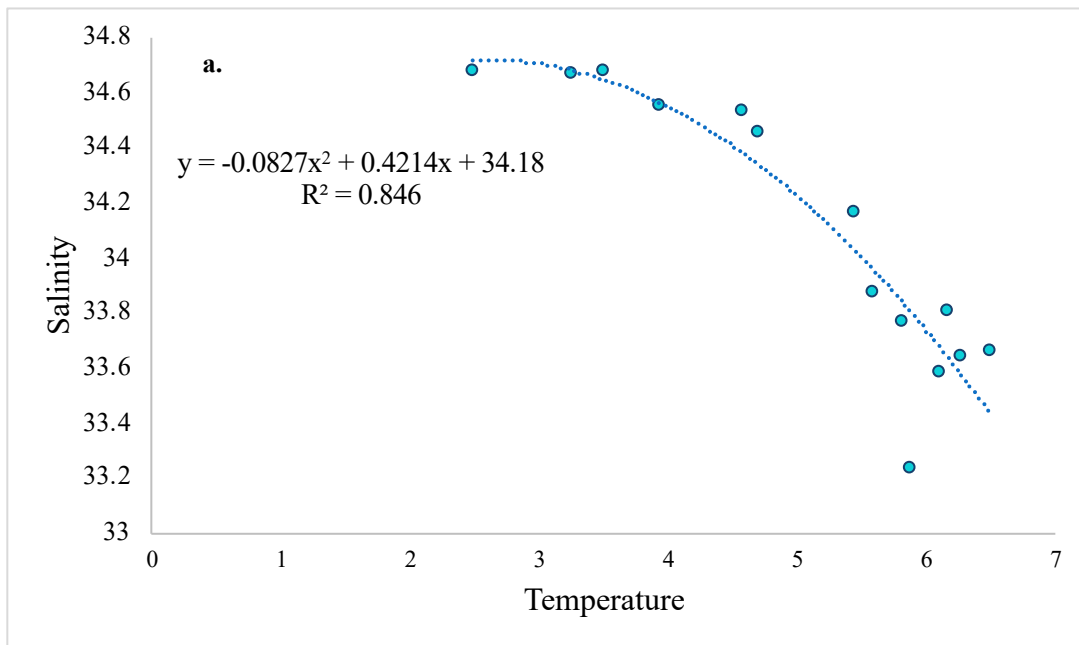
629

630

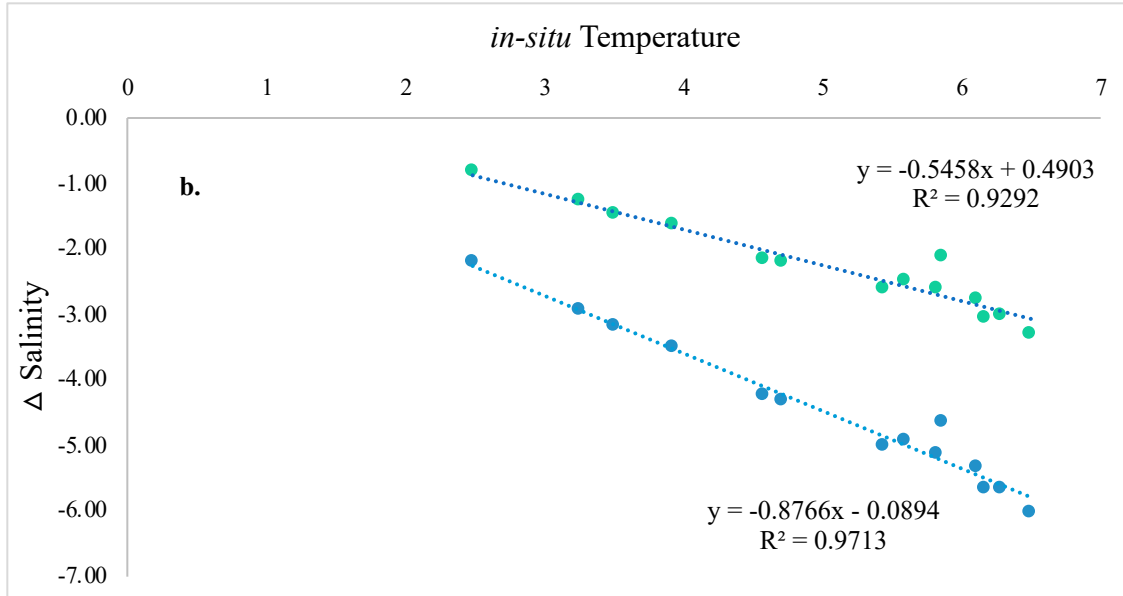
631 **Appendix**

632 **A1. Calculation of Salinity Offset**

633 In the summer of 2020—weeks 22 to 35— the mean temperature at 11 m displayed a range from  
634 2.48 – 6.28, with salinity values ranging from 34.67 measured at the minimum 2.48°C and 33.63  
635 measured at 6.28°C (Fig. A1a). The correlation was best fit with a 2<sup>nd</sup> order polynomial. To  
636 project the salinity offset at a future temperature based on this 2<sup>nd</sup> order polynomial fit,  
637 temperatures of + 3.3 and 5.3°C (SSP2-4.5 and SSP5-8.5, respectively) were added to *in-situ*  
638 fjord temperatures and salinity was calculated based on the 2<sup>nd</sup> order polynomial. These  
639 estimated salinity values were then subtracted from the mean salinity values observed (y-axis,  
640 Fig. A1a) in summer 2020 in order to calculate a delta salinity value for the SSP2-4.5 and SSP5-  
641 8.5 scenarios. The relationship between these estimated delta salinity values and the mean *in-situ*  
642 temperature (y-axis, Fig. A1a) displayed a robust linear relationship (Fig A1b).



643



644

645 **Figure A1.** Relationship between temperature and salinity in summer 2020 weeks 22 – 35 in Ny-  
 646 Ålesund, Svalbard (a). Relationship between estimated delta salinity and *in-situ* temperature,  
 647 where delta salinity was calculated as the difference between the current mean salinity and the  
 648 salinity estimated at the temperature increase projected for SSP2-4.5 (green dots) and SSP5-8.5  
 649 (blue dots) scenarios (b).

650

651

652

653

654

655

656

657

658

659

660 **Table A1. Parts list with manufacturer model numbers.**

Group	Item	Supplier/manufacturer	Model / details	Quantity
<b>Hydraulic system</b>				
	Mesocosms	home made	1000 L fiber glass	12
	Seawater pump	NPS, BradFord, UK	Albatros F13T	1
	PVC-U tubing and fittings		20mm, 32mm & 50mm diameter	—
	Insulated flexible hose		19mm diameter	100 m
<b>Sensors</b>				
	Conductivity / temperature	Aqualabo, Champigny sur Marne, France	PC4E	12
	Oxygen	Aqualabo, Champigny sur Marne, France	PODOC	12
	Pressure	Siemens, Munich, Germany	7MF1567-3BE00-1AA1	3
	Flow rate	IFM, Essen, Germany	SV3150	12
<b>Actuators</b>				
	Pressure regulation valves	BELIMO, Hinwil, Switzerland	R2025-10-S2 with LR24A-SR motor	3
	Temperature regulation valves	BELIMO, Hinwil, Switzerland	R3015-10-S2 with LR24A-SR motor	12
	Salinity regulation valves	BELIMO, Hinwil, Switzerland	R2015-10-S2 with LR24A-SR motor	6
<b>Automation cabinet</b>				
	Cabinet	Fibox, Espoo, Finland	FIB8120017N	1
	Security switch	KRAUS-NAIMER, Karlsruhe, germany	KNA002245	1
	12 vdc power supply	TDK Lambda, New York, USA	LAMDRL30-12-1	1
	24vdc power supply	TDK Lambda, New York, USA	LAMDRB240-24-1	1
	PLC	Industrial Shields, Barcelona, Spain	Mduino-42+	4
	Ethernet switch	HIRSCHMANN-INET, Neckartenzlingen, Germany	HIR942132002	1

## 662 **A2. Temperature and Salinity Regulation**

663 Accurate temperature and salinity regulation was managed using the software PID (proportional  
664 integral derivative) controller on the corresponding Programmable Logic Controller (PLC). The  
665 PLC operated in PoE mode (power over ethernet) which builds a local area network (LAN)  
666 enabling use of Ethernet data cables to carry electrical power. The PID controller measures the  
667 difference between the measured value and the nominal value (i.e., the error). This calculates the  
668 position and adjustment of the valve opening by multiplying the error, the integral of this error,  
669 and the derivative of the error over time, by previously determined coefficients  $K_p$  (proportional  
670 gain),  $K_i$  (integral gain) and  $K_d$  (derivative gain), respectively. These coefficients were obtained  
671 experimentally using the empirical method of Ziegler & Nichols (1943). These coefficient values  
672 may differ from one condition to another.

673

### 674 **A2.1. Pressure and Flow Regulation**

675

676 Each sub-header tank inlet line of ambient, chilled and warmed seawater had its own pressure  
677 regulation system enabling equivalent pressure levels to be maintained. This regulation process  
678 aided in the ability to adjust flow rates for all mesocosms by using the hand-crank valves (Fig.  
679 1). The system consisted of an analog pressure sensor (Siemens© 7MF1567-3BE00-1AA1) and  
680 a two-way analog valve (BELIMO© R2025-10-S2 with LR24A-SR motor). The pressure  
681 sensors were placed in-line directly after water from each sub-header tank passed through a  
682 regulator valve. The sensor ensured that pressure for each line was maintained at 0.3 bars by  
683 transmitting data to the system which then regulated the valve opening position of the incoming  
684 flow. A nominal pressure for all three sensors was predetermined during flow rate test trials. This



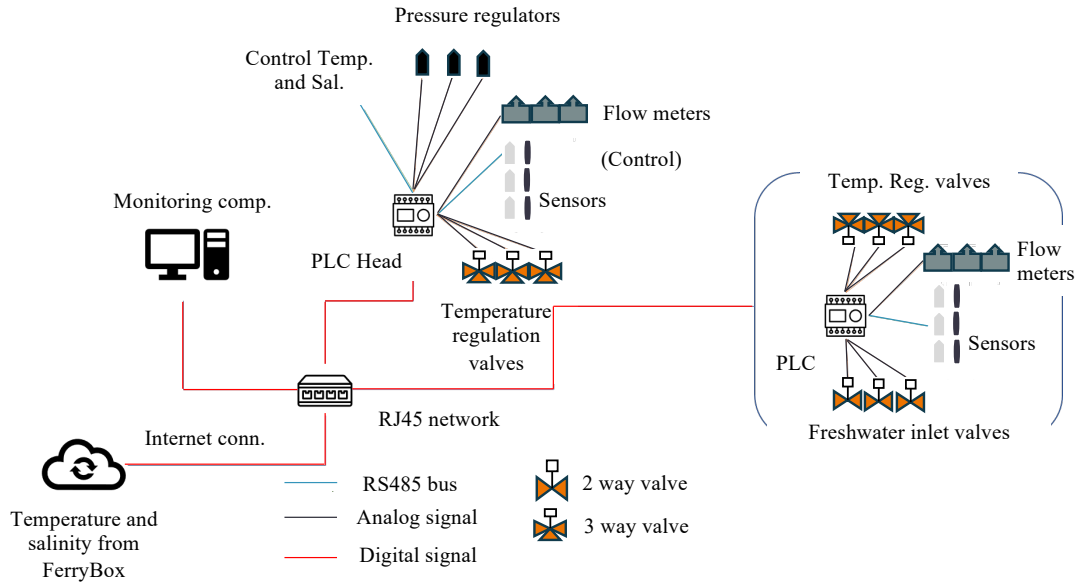
685 process took place during the setup of the system where the valve opening was adjusted using a  
686 PID regulator (see A2) to maintain the defined nominal pressure.

687  
688 **A2.2 Automation**

689 The automation was performed using 4 Industrial Arduino-based PLCs (Industrial shields©  
690 Mduino-42+), with an individual PLC regulating the control and each treatment 1 – 3,  
691 respectively. Each PLC was responsible for logging data and regulating a specific experimental  
692 condition. The PLC regulating the control—identified as the Head PLC—was the primary device  
693 responsible for communication with the branched PLCs and the monitoring computer (Fig. A2).  
694 All monitoring was performed on a PC Windows application (Section A3) and responsible for:  
695 (1) reading data received from the PLCs, (2) reading *in-situ* data received from the internet, (3)  
696 displaying live data, (4) logging data and sending it to an FTP server, and (5) sending settings  
697 and commands to the PLCs. Communication between the PLCs and the PC was ensured using  
698 http WebSocket protocol on RJ45 ethernet cables. The communication between the PLCs and the  
699 conductivity-temperature and oxygen sensors, flow rate sensors, and regulation valves was  
700 executed using a half duplex RS485 (2 wires) protocol, with an analog 4-20mA and an analog 0-  
701 10V signal, respectively. All PLCs and wired communication lines were housed in an electrical  
702 box installed to an IP68 Fibox enclosure with a 400 V (3P+N+E) 32 A security switch (Fig. A6).  
703 All the automation elements use low tension (12 Vdc or 24 Vdc) through circuit breakers and  
704 fuses. The electrical box was protected with a 220 V socket.

705

# Automation Hardware Architecture



706

707 **Figure A2.** Diagram and flow-chart of the automation system.

708

709

710

711

712

713

714

715

716

717

718

719 **A3. Software Development**

720 The code for the application was written in C/C++. The code uses publicly available Arduino  
721 libraries (<https://www.arduino.cc/reference/en/libraries/>) as well as originally designed libraries.  
722 All code is available on Github (<https://github.com/purrutti/FACEIT>). The code is divided into  
723 two pathways: ‘Master.ino’ for the Head PLC, and ‘Regul\_condition.ino’ for the Branched  
724 PLCs. A description of the main functions applied in the code for programming the system  
725 regulation and features are listed in Table A3.

726

727

728

729

730

731

732

733

734

735

736

737

738

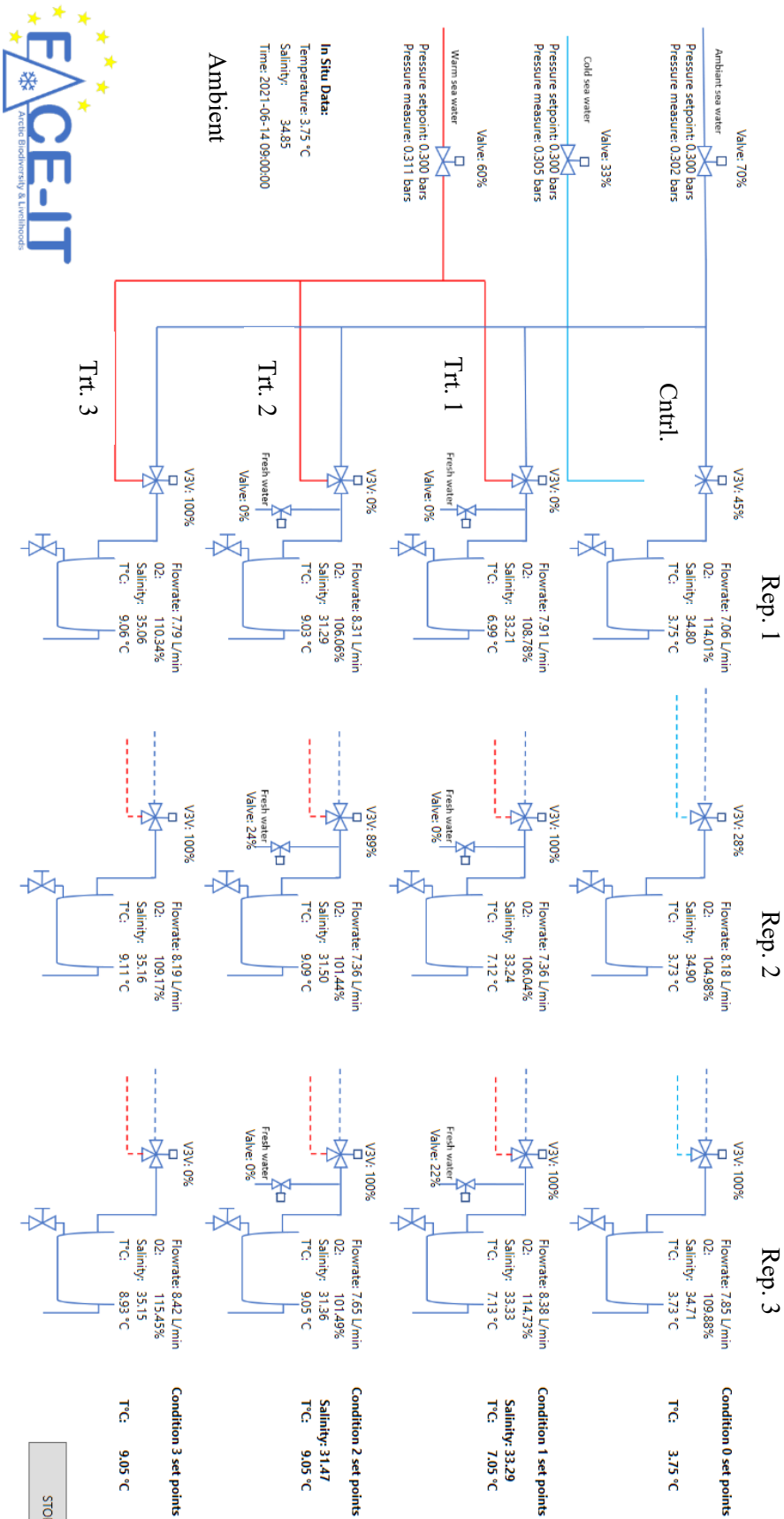
739

740

741

742 **Table A3.** Functions used for programming of software.

Function	Operation	Arcellery field Sender ID	Arcellery field Command #
<i>RTC/read()</i>	The PLCs are equipped with a RTC chip and battery to keep track of the date. Once set on commissioning, <i>RTC.read()</i> returns the current date and time. This function loops through each sensor connected on the RS485 bus. Each Mesocosm has two sensors (O2 and Conductivity/Salinity), so each PLC has 6 sensors connected on its bus.		
<i>readMesosensors()</i>	- O2 sensors have addresses ranging from 10 to 12, for mesocosms 0 to 2 of the scenario, respectively. - PC4E sensors have addresses ranging from 30 to 32, for mesocosms 0 to 2 of the scenario, respectively. - Sensors are requested individually and in sequence. A request is made every 200 ms.		
<i>websocket/loop()</i>	This is a callback function responsible for dealing with the WebSocket communication. The master PLC is the WebSocket server. It listens to slave PLCs requests and to the monitoring PC requests. Requests are JSON formatted. They always contain <i>entityId</i> / <i>fields</i> : <i>senderID</i> (ID of the entity sending the request), <i>condID</i> (ID of the requested entity), <i>command</i> (command type of the request). They optionally can also contain a « <i>time</i> » field: Unix-like timestamp (number of seconds since 01-01-1970)	Head PLC (ID = 0) Branched PLCs (ID = 1-3) Monitoring PC (ID = 4)	Request params: <i>sepoints</i> , PID settings (# = 0) Request data: measurement values, regulation outputs (# = 1) Send Params: response to a « request params » request (# = 2) Send Data: response to a « request data » request (# = 3) Calibrate sensor: request for calibrating sensor to specified value (# = 4) Request Head data: specific data measured by Head PLC (pressure & flowrates) (# = 5) Send Head data: a response to a « request Head data » request (# = 6)
<i>regulationTemperature()</i>	This function is responsible for the temperature regulation of the mesocosm. It sets the corresponding three-way valve position using a 0-10V analog signal. The function first checks if the regulation is in « manual override » mode. If so, it applies the override setpoint. If not, it reads the temperature measure in the mesocosm, compares it with the setpoint, and uses the PID settings to set the valve position.		
<i>checkMesocosms()</i>	This function loops through every mesocosm every 200 ms and reads analog signals (i.e., flowrates and pressure readings).		
<i>regulationPressure()</i>	This function is responsible for the pressure regulation of the mesocosm. It sets the corresponding three-way valve position using a 0-10V analog signal. The function first checks if the regulation is in « manual override » mode. If so, it applies the override setpoint. If not, it reads the pressure measure in the mesocosm, compares it with the setpoint, and uses the PID settings to set the valve position.		
<i>printOASD()</i>	Master PLC is equipped with a microSD card, on which data from all mesocosms is logged every 5 seconds, in one csv file per day. This is for security only, as the microSD card is not easy to remove from the PLC casing. It should not be removed before the end of the experiment.		
<i>regulationSalinite()</i>	This function is responsible for the salinity regulation of the mesocosm. It sets the corresponding three-way valve position using a 0-10V analog signal. The function first checks if the regulation is in « manual override » mode. If so, it applies the override setpoint. If not, it reads the salinity measure in the mesocosm, compares it with the setpoint, and uses the PID settings to set the valve position.		
<i>Only for Branched PLCs</i>			



745 **Figure A3.** Application interface displaying real-time monitoring of ambient conditions as well  
746 and control (Cntrl.), and treatment (Trt.) conditions for each replicate (Rep.) in each mesocosm.

747

748

749

750

751

752

753

754

755

756

757

758

759

760

761

762

763

764

765

766

767

#### 768 **A4. Menu bar of PC application**

769 From the interface, the user sets the temperature condition and associated salinity offset, IP  
770 address and logging parameters, sensor calibration settings, and nominal pressure (Fig. A4).

771 Within the menu bar several tabs permit the setup of the project: file, settings, maintenance, and  
772 data. Under ‘file’ the system can be manually connected to, or disconnected from, the PLCs.

773 Connection is usually maintained automatically. The ‘settings’ tab displays the application and  
774 experimental setting options (Fig. A4.1 a – c). All the settings of the project are stored on the  
775 computer (found in ‘application settings’) that is running the application, which include:

- 776 i. *Master IP address*: The IP Address of the Master PLC (centralizing all the data).
- 777 ii. *Data Query Interval*: Frequency of queries from the application to the master PLC.
- 778 iii. *Data Log Interval*: Number of minutes between logs to file.
- 779 iv. *Data Base File Path*: Directory and base filename of the csv data files.
- 780 v. *FTP Username, Password, Path*: FTP settings for sending the data file every hour.
- 781 vi. *InfluxDB Settings*: For Live Monitoring and local storage of the data.

782 Under ‘experimental settings’, the programmed specificities and regulation of the treatment  
783 conditions can be adjusted. This includes programming the nominal pressure (all main inflow  
784 lines), temperature and the salinity-temperature relational equation (on a different tab selected  
785 from dropdown), as well as adjusting the  $K_p$ ,  $K_i$  &  $K_d$  coefficients for the regulation (see section  
786 2.3.1). The nominal temperature is provided by the data received from the ferry-box, however  
787 this can be overridden if needed. The « Save to PLC » button sends the values to the  
788 corresponding PLC and saves the data, while the « Load from PLC » button loads the settings  
789 from the PLC. For the purposes of this experiment, the nominal salinity was calculated based on  
790 a delta salinity for treatments 1 and 2 which were derived from the linear relationship with

791 temperature (see section 2.3.1). This can also be overridden if needed by selecting the manual  
792 override box.

793         The ‘maintenance’ tab is where sensor calibration and communication ‘Debug’  
794 operations can be executed (Fig. A4 d, e). Calibration can be performed for each sensor deployed  
795 in each mesocosm, and uses a 2-point calibration for temperature and % oxygen. The salinity  
796 calibration is done by setting the conductivity value corresponding to a temperature of 25°C  
797 rather than the *in situ* measured temperature. The conductivity value is programmed as  $\mu\text{S cm}^{-1}$ .  
798 The communication process for sensor calibration is between 5 to 10 seconds. The final option in  
799 the menu is the ‘data’ tab which displays the historical and live data. The historical data can be  
800 interfaced to an html site if desired.

801



### 2. a.

Master IP address: 172.16.33.10  
Data Query Interval: 1  
Data Log Interval: 5 minutes  
Data Base Request: C:\Control\FACET\NMS\_Memo\_Epp

**FTP**  
 Username: ocontrol  
 Password: OGC0hC@201  
 FTP Directory Path: ftp://ms-wi-fi/FACET/Data\_FACET/

**Hardware**  
 Webpage: http://localhost:8080/cgi-bin/kefct176k417714mbkwdt715110000007bwerzmv4281237450\_36701  
 Token: e4ND9pwad56g9b0c6kwt-Q3hucd5V0cawv9u4G9JzIvz0Lc-c7HhLJn08L3hw-dAm4Zc4kdyg==  
 Bucket: FACET  
 Org: OMS

Save Cancel

### b.

**Experiment Settings**

Control Condition:

**Pressure regulation**

Pressure setpoint:

Kp:   
 Ki:   
 Kd:

Manual Override:  %

**Temperature regulation**

Temperature setpoint:

Kp:   
 Ki:   
 Kd:

Manual Override:  %

Load from PLC Save to PLC Cancel

### c.

**Experiment Settings**

Condition 1

**Salinity regulation**

delta Salinity =  x Ambient T°C +

delta Salinity setpoint:   
 Salinity setpoint:

Kp:   
 Ki:   
 Kd:

Manual Override:  %

**Temperature regulation**

delta T°C setpoint:   
 Temperature setpoint:

Kp:   
 Ki:   
 Kd:

Manual Override:  %

Load from PLC Save to PLC Cancel

### d.

**Calibration**

CO:  Measurement:

Temperature:

Set Offset:  Ideally a value between 0°C and 5°C  
 Set Slope:  Ideally a value between 20°C and 25°C

Factory/reset

Please be patient. The calibration process can take a while. If the measure is not updated after 30 seconds, you are allowed to re-click on the button. (otherwise a double click does the trick)

### e.

**Communication Debug**

Request sent:  
 ["command":1,"condID":0,"senderID":4]

Response received:  
 [{"command":3,"condID":0,"senderID":0,"time":1623882025,"data": [{"MID":0,"temp":3.71153,"cond":5281837,"sal":34.81795,"flow":7139935,"sasPID\_pc":53,"tempSPID\_pc":100,"oxy\_pc":113.54461}], [{"MID":1,"temp":3.717137,"cond":5289236,"sal":34.87269,"flow":7298964,"sasPID\_pc":115,"tempSPID\_pc":100,"oxy\_pc":104.17221}], [{"MID":2,"temp":3.737186,"cond":5287632,"sal":34.71262,"flow":71628548,"sasPID\_pc":82,"tempSPID\_pc":100,"oxy\_pc":109.51521}], [{"MID":3,"temp":3.737186,"cond":5287632,"sal":34.71262,"flow":71628548,"sasPID\_pc":82,"tempSPID\_pc":100,"oxy\_pc":109.51521}], [{"MID":4,"temp":3.737186,"cond":5287632,"sal":34.71262,"flow":71628548,"sasPID\_pc":82,"tempSPID\_pc":100,"oxy\_pc":109.51521}]}]

803 **Figure A4.** Operation windows for the application and experimental settings (**a-c**). These  
804 windows are found under the ‘settings’ tab. Operation windows for sensor calibration and  
805 debugging (**d, e**). These are found under the ‘maintenance’ tab.

806

807

808

809

810

811

812

813

814

815

816

817

818

819

820

821

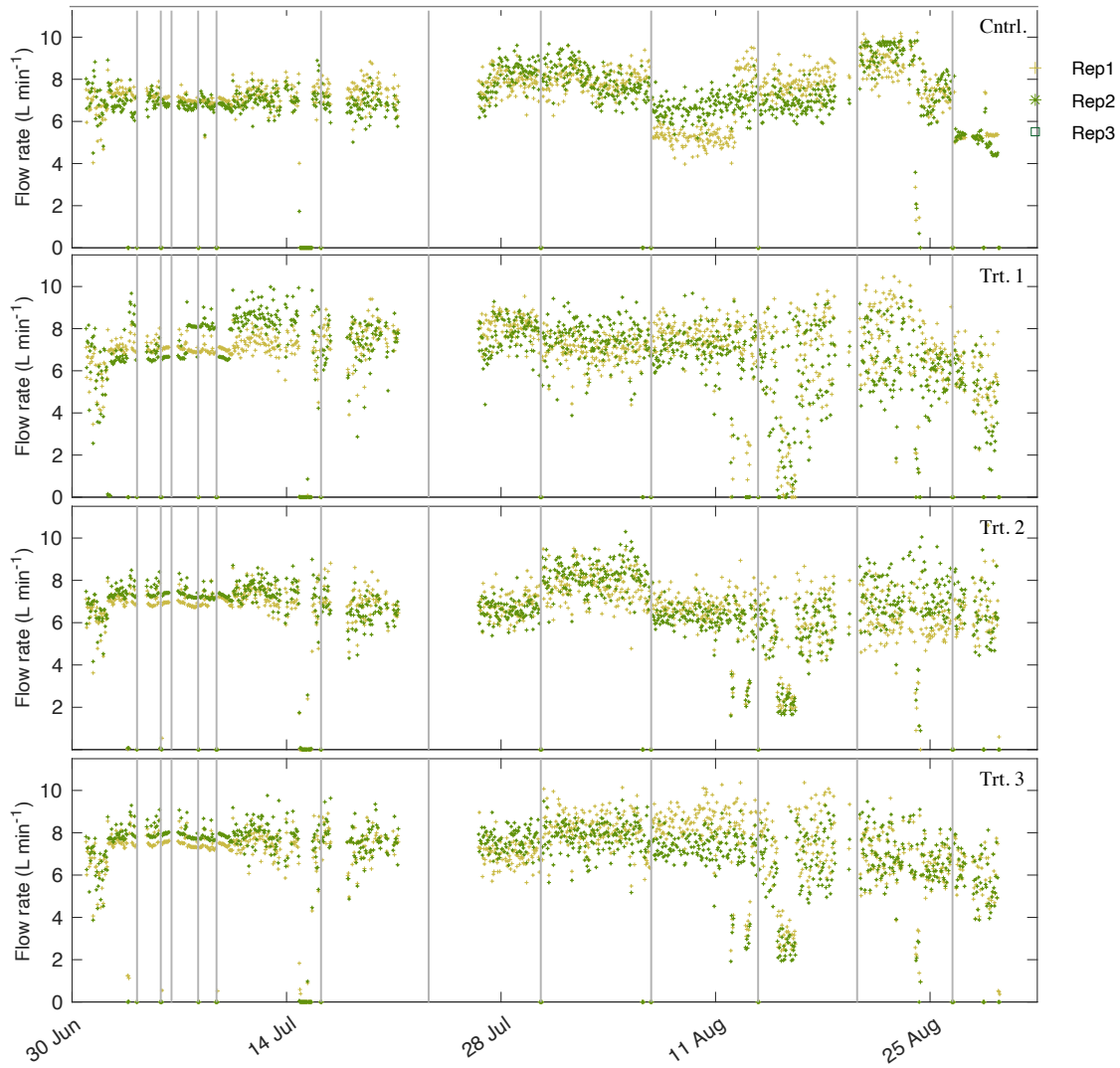
822

823

824

825

826



827

828 **Figure A5.** Flow rates for control and treatments 1-3 for the entirety of the system deployment.

829 Black vertical lines are when incubations were performed and the system shut-off for a period of

830 3 h. Flow rates went to zero at these times.

831

832

833

834



835

836 **Figure A6.** All 12 mesocosms are displayed (upper left photo) with the inside of one mesocosm

837 (right photo) showing the oxygen (silver) and temperature/conductivity sensors along with the

838 photosynthetically active radiation (PAR) logger (bottom right photo).

839

840

841

842

843

844



845

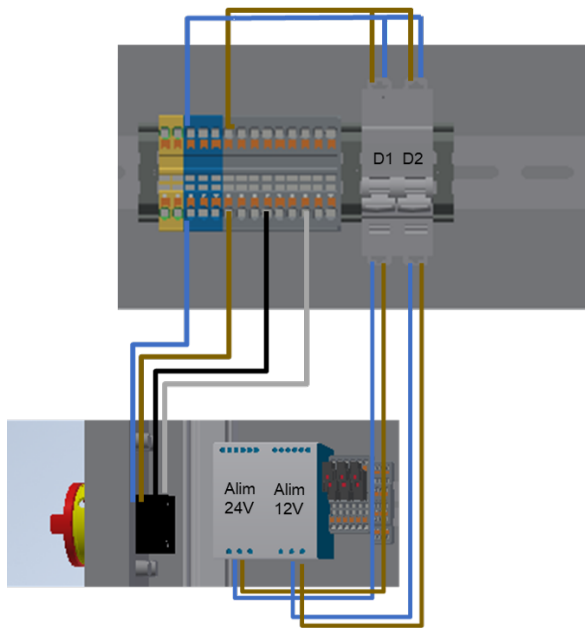
846 **Figure A7.** Electrical cabinet used for SalTExPreS

847

848

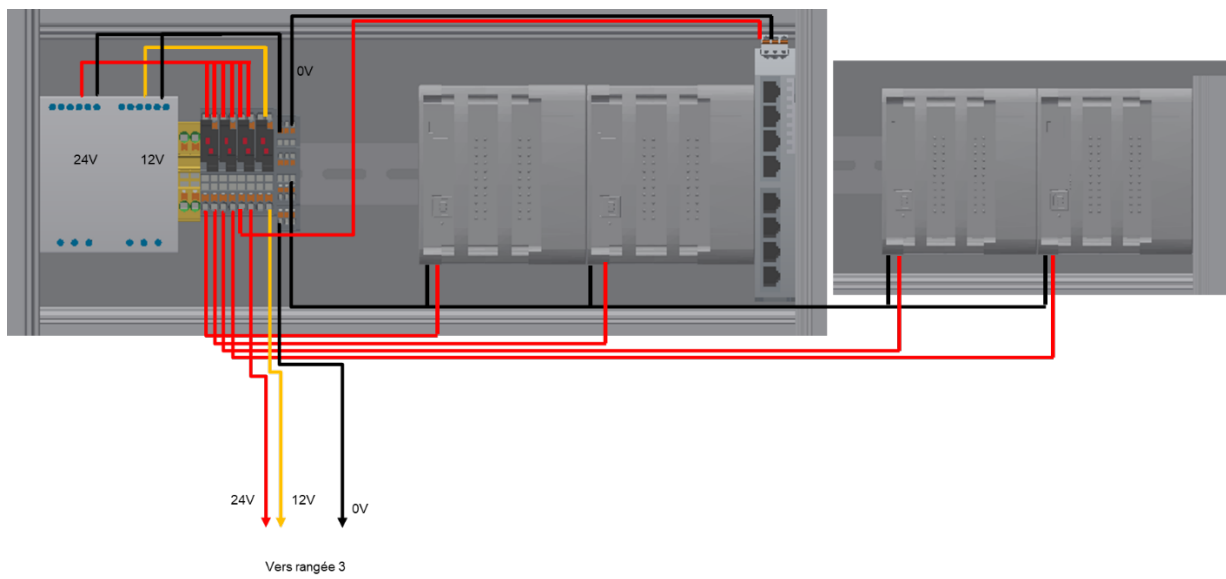
849

850



D1: Alim 24Vdc  
D2: Alim 12Vdc

851



852

853 **Figure A8.** Electrical schematic for wiring within the electrical box.

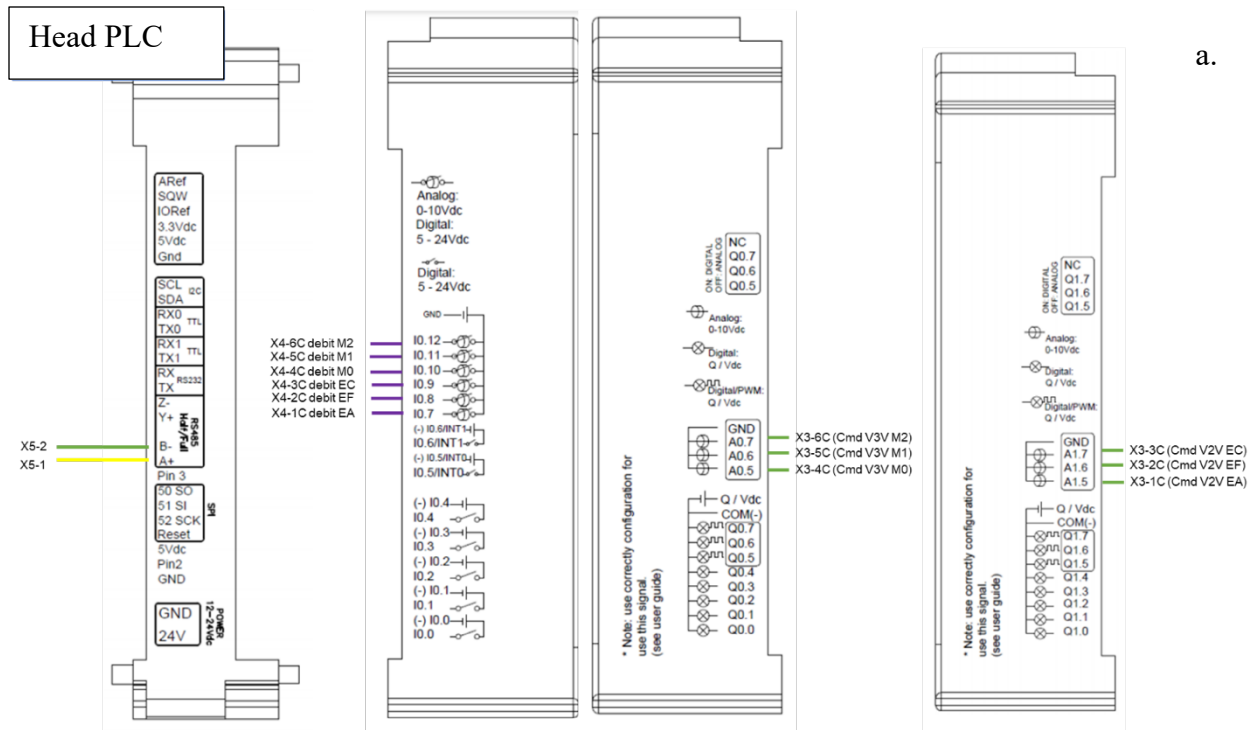
854

855

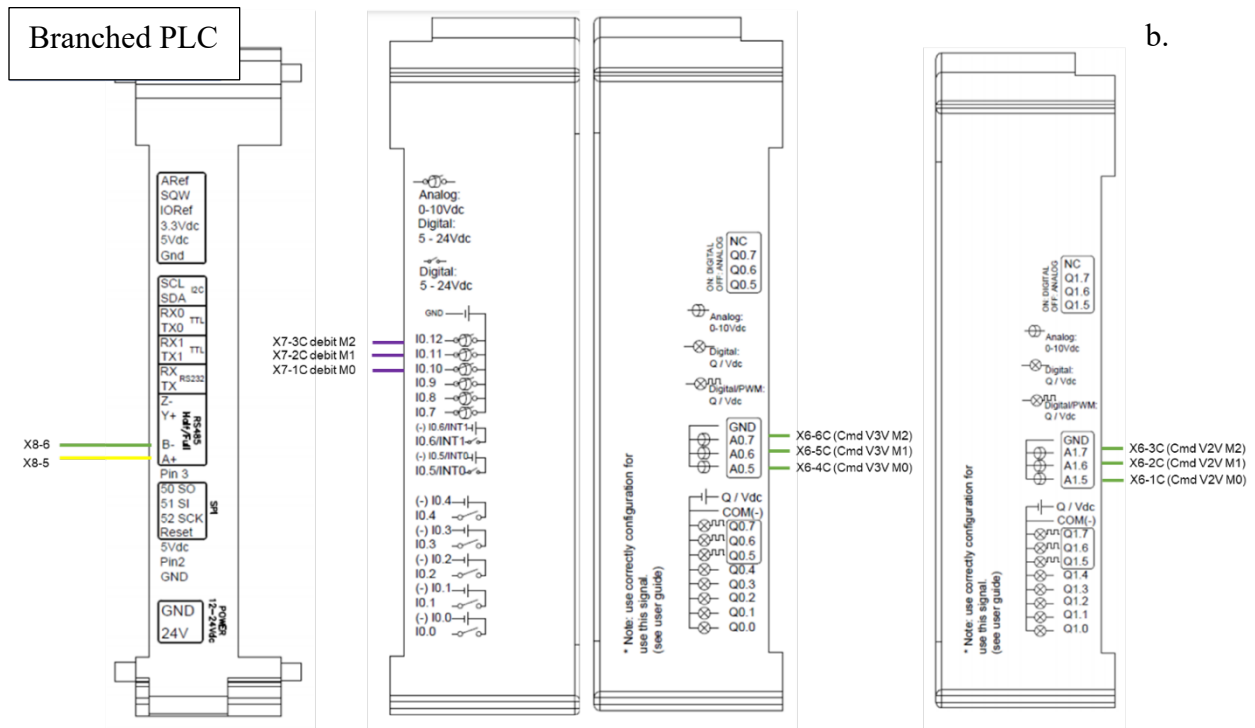
856

857

858



859



860

861 **Figure A9.** PLC controller diagram for Head (a) and Branched (b) operations.

862

863